A COMPUTER SIMULATION MODEL FOR COMPLIANT MECHANISM FOR BIO-MIMETIC FISH

G. Govindarajan
Bio-mimetic Propulsion Laboratory
Department of Ocean Engineering, IIT Madras
Chennai (TN) - 600036, India
ggovindarajaniit@gmail.com

R. Sharma
Bio-mimetic Propulsion Laboratory
Department of Ocean Engineering, IIT Madras
Chennai (TN) - 600036, India
rajivatri@iitm.ac.in

***Abstract*–This paper presents a computer simulation model to study the bio-mimetic fish modeled as a compliant beam. The aim is to determine the natural frequencies of the fish and then compute and characterize the mode shapes and relate them to propulsive thrust. The application of model is focused on design of propulsion systems with compliant bodies for bio-mimetic locomotion in marine environments. The compliant bodies are designed for their natural frequency modes (i.e. the mode that most resembles the desired kinematics) and since they operate in the matching range of natural frequencies they are energy efficient. In the model fish is assumed as a bio-mimetic compliant beam of a varying cross sectional parameters and 'Timoshenko Beam (TB)' theory is used in the computer simulation model to compute mode shape and thrust. The presented results clearly establish the mode shape and the resultant thrust.**

***Index Terms* - Smart complaint mechanism, bio-mimetic propulsion, compliant beam, cantilever beam, sensors.**

I. INTRODUCTION

The present work is motivated from the promising features of natural biology inspired (bio-mimetic) mechanisms. These ideas can be utilized to address the limitations of traditional propeller driven mechanisms. A recent research interest has been to combine the bio-mimetic designs with the use of compliant structures for underwater locomotion [1].

The main premise is that the nature offers remarkable choices for propulsion with extra ordinary efficiency, e.g. fish depends on aquatic agility for its survival and can reverse direction without slowing down and with a turning radius that is only 10 to 30 percent of the length of their bodies. For comparison, maneuvering ships must reduce their speed by more than 50 percent and their turning radius is at least 10 times larger than the corresponding, value for fish [2]. Because of their inherent advantages, in recent times, the interest in mimicking approaches from natural biology has increased in order to ameliorate performance of man-made mechanisms in the marine environments.

The motivation behind this paper is to explore a computer simulation model to study how a bio mimicking approach can be simulated? We present a computer simulation model to study the bio-mimetic fish modeled as a compliant beam. Our aim is to determine the natural frequencies of the fish and then compute and characterize the mode shapes and relate them to propulsive thrust. The application of model is focused on design of propulsion systems with compliant bodies for bio-mimetic locomotion in marine environments. We assume the fish as a bio-mimetic compliant beam of a varying cross sectional parameters and use 'Timoshenko Beam (TB)' theory.

The architecture of computer simulation model is modular and though the various modules are integrated in simulation model they can be computed independently. The modules can be added and that will be investigated later in future. Our presented results clearly establish themode shape and the resultant thrust.

II. SMARTCOMPLAINT MECHANISM

The 'Compliant Mechanism (CM)' has an elastic pair and elastic segment and it uses the elastic deformation to transmit or transform force, motion, energy and/or a combination of these. It is designed to accomplish with a one-piece device what conventional mechanisms can do with multiple pieces. Unlike rigid-body mechanisms, which achieve their motion from kinematic pairs or joints allowing motion in one or more directions, the members incompliant mechanisms provide energy storage along with their motion. A CM is designed to be flexible enough to transmit motions and at the same time stiff enough to withstand the external loads. Structurally, the hinge-less nature of CM eliminates the backlash error and effectively reduces the production and maintenance costs associated with the multiple pieces assembly.

978-0-933957-43-5 ©2015 MTS

In our design the fish is assumed as a compliant beam and is modeled as a 'Timoshenko Beam (TB)' with non-uniform cross-section actuated by a time varying moment. The method of assumed modes is used to derive the equations of motion of the fish and to find a relationship between the applied force in the smart material and the resulting lateral deflections. And, our aim is to develop the equation of dynamics of bio-mimetic fish and find the relationship between the applied force and the resulting kinematics.

A. Role of Smart Material and Sensor

In 'Macro Fiber Composite (MFC)' - a type of piezo-fiber material - an applied electrical field induces a mechanical strain in the material and this phenomenon can be used in the design of different types of actuators depending upon the requirements. However, though simple in theory it is difficult to achieve in practice. Because of this reason there has been very little research on piezoelectric actuation to swimming and its application in underwater vehicle design. From hydrodynamic point of view, the fish tail is driven through a mechanism that is actuated by the bending of two curved beams.

In our application a piezoelectric actuator drives a stroke amplifying compliant mechanism. In this arrangement CM sacrifices output force for the increased stroke generation and thus output deflection decreases significantly when loaded. When the reduced force is coupled with the effects of added mass associated with the compliant mechanism itself, as well as the added effective mass of a displaced fluid, it results into low amplitude fin deflection and slow vehicle velocities. In our application, we need discrete motion amplifying mechanism by employing high deflection bending MFC actuators, whose piezo-stroke amplification into large output deflections is integral to the actuator design. The motivation for using bending piezoelectric actuators in our application - in addition to their inherent motion amplification - is the linear oscillatory motion they exhibit when subjected to a sinusoidal voltage which is the analog of the motion a caudal fin exhibits during thrust generations.

III. GOVERNING EQUATIONS OF SIMULATION MODEL

In our simulation model the fish is assumed to be a continuous compliant beam with a non-uniform cross section and is actuated by a time varying moment applied at a distance 'x_2'. This time varying applied moment is utilized in introducing desired bending in the beam. The schematic of fish as a continuous Timoshenko beam (TB) with Compliant Mechanism (CM) is shown in Fig. 1. We use the TB theory in which the cross sections remain planar and rotate about the same neutral axis as the Euler-Bernoulli model, but do not remain normal to the deformed longitudinal axis. The deviation from normality is produced by a transverse shear that is assumed to be constant over the cross section. The total slope of the beam in this model consists of two parts: 1) Due to bending , and 2) Due to shear . The application of TB theory in fish like propulsion implies that the propulsion will be a function of both time and location (Coordinates).

Following[3], the mathematical equation of TB is:

$$\mathrm{EI}\,\frac{\partial^4 f}{\partial x^4} + \rho\mathrm{A}\,\frac{\partial^2 f}{\partial t^2} - \rho\mathrm{I}\left(1+\frac{E}{kG}\right)\frac{\partial^4 f}{\partial x^2 \partial t^2} + \frac{\rho^2 I}{kG}\,\frac{\partial^4 f}{\partial t^4} + Cd\,\frac{\partial f}{\partial t} + 0.5Cd\,\frac{\partial f}{\partial t}\,\frac{\partial f}{\partial t}\,\rho\mathrm{A} = 0 \quad \ldots\ldots\ldots\ldots (1a)$$

$$\mathrm{EI}\,\frac{\partial^4 \psi}{\partial x^4} + \rho\mathrm{A}\,\frac{\partial^2 \psi}{\partial t^2} - \rho\mathrm{I}\left(1+\frac{E}{kG}\right)\frac{\partial^4 \psi}{\partial x^2 \partial t^2} + \frac{\rho^2 I}{kG}\,\frac{\partial^4 \psi}{\partial t^4} + Cd\,\frac{\partial \psi}{\partial t} + 0.5Cd\,\frac{\partial \psi}{\partial t}\,\frac{\partial \psi}{\partial t}\,\rho\mathrm{A} = 0 \quad \ldots\ldots\ldots\ldots (1b)$$

In Equations (1a&1b), E is the Young's Modulus (N/m^2), I is the sectional area moment of inertia (m^4), k is the shear correction factor, fis the deflection of beam (m), and ψ is the shear deformation of beam.

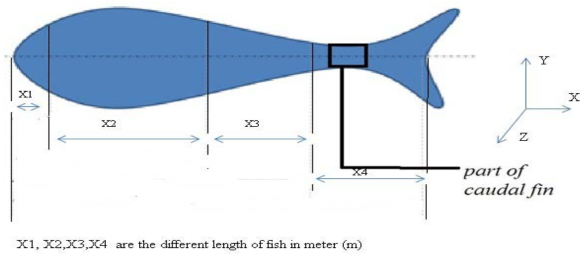

Fig. 1: The schematic of fish as a continuous CM - TB

IV. EFFECT OF SHEAR DEFORMATION

Using TB theory - Equations (1a and 1b) - the effect of shear deformation upon natural frequencies of a cantilever beam with varyingsection properties can be estimated and the terms provide the correction factor due to shear and rotary inertia for a cantilever beam. The term of correction factor accounts for two important effects: 1) Effect of shear deformation for the principal effects of rotary inertia, and 2) effect of shear deformation.In casesof beams having varying section properties the natural frequencies are characterized by the moment of inertia Iand modulus of elasticity E.

V. PRINCIPLE OF PROPULSION IN BEAM

In the mechanics of fish motion, the fish is assumed as a CM-TB and the driving force generated in cantilever beam is thepropulsion of system. This driving force is related to the MFC and we assumed the fish has a non uniform cross section with variation in moment of inertia and Young's modulus. The external force of the MFC changes with time and the drag force dependon position of the beam. The propulsion or thrust generated is a function of both time and coordinate.

Following [4-5], the variation of Young's modulus and moment of inertia along the CM – TB can be expressed:

$$I = I_o\left(1 + c_1 X\right), \text{ and} \quad (2)$$

$$E = E_o\left(1 + c_2 X\right) \quad (3)$$

wherec_1 and $c_2$are the variation of cross sectional properties of fish and $0 \leq c \leq 1$;A is the area of cross section in m^2; I is the moment of inertia in m^4;E is the modulus of Elasticity N/m^2; L is the distance of center of inertia from the trailing edge. Similar to the material uses in [1], the variation of elastic modulus is assumed between 4.574E5 to 7.964E5 and the inertial response is based on combined inertia of fish and water ($m+m_f$), [6-7]. Now, our moment formulation is:

$$M = \int_0^l \left(m + m_f\right) dx, \quad (4)$$

$$ML = \int_0^l \left(l - x\right)\left(m + m_f\right) dx, \text{ and} \quad (5)$$

$$I_m = \int_0^l \left(l - x\right)^2 \left(m + m_f\right) dx \quad (6)$$

where ML is the moment of robotic fish with respect to the center of body, M is the mass of the fish; I_m is the mass moment of inertia of the robotic fish in Kg-m^2. In our work, the moment of inertia varies in between 8.48275E-6and 6.5E-5.The factors influencing propulsion include material, size of the beam (primary dimension and cross sectional distribution of area) and viscosity of the liquid [8]. The boundary conditions for the cantilever TB are: f(0)=0, f'(0)=0, f''(0)=0, and f'''(0)=0. The distribution of force due to piezoelectric effect of the beam (i.e. external excitation) has an impact on the vibration modes and the propulsion.

VI. RESULTS AND DISCUSSION

(A) Without smart material

The characteristic modes of non-uniform cross section of fish idealized as a TB and the computed amplitudes of these six modes of lateral movements from head to tail are shown in Figs. 2 to 17. After computing the characteristic modesof the non-uniform TB, we compute the thrust (force) generated by theMFC element. This generated thrust (force) depends upon both the material and geometric properties of the actuators and TB. While a fish swims, the energy is captured through the bio-physical process of muscle contraction, this energy is transferred to tail through bending motion or un-dulatory motion or oscillatory/flapping and/or a combination of these. This or these motion/s of tail can produce thrustdepending upon the modes of swimming. Bio-mechanically, the early stage of swimming is dominated by the first mode shape [8-9] and this corresponds to the fish oscillating only its tail. Later, the second mode of oscillation dominates the rest of swimming process and the maximum amplitudeof vibration of fish is 0.12m. The E varies from 5.05825E5 to 7.96395E5 and theproper placement of MFC patch can be identified by the root locus analysis because it is based upon bi-morph system.

VII. SIGNIFANCE OF MODE SHAPE AND PHASE DIFFERENCE

The mode shape is related to the stage of propulsion. The early stage of propulsion is in the first mode and the sequential bendingmode shape of the fish body plays an important role in generation of thrust and attaining higher efficiency. The amplitude and phase difference provide critical information about the stability of propulsion of robotic fish and condition of maneuverability. The phasedifference information in mode shape is important to studythe dynamic mechanism of fish propulsion and to analyze the trend of initial startup of fish, idealistic motion of the fish andquick and highly maneuverable motion of fish.A phase study is a collection of phase information made on a fish and is evaluated to reveal information about the amplitude and natural frequency. Figs. 2 to 17 show the difference in phase information of the fish and respective mode shape of the fish.

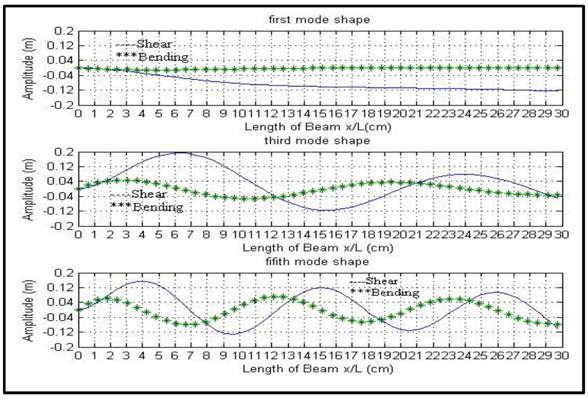

Fig. 2: The modes of vibration of fish with Young's modulus (4.5175E5) and moment of inertia (8.48275E-6)

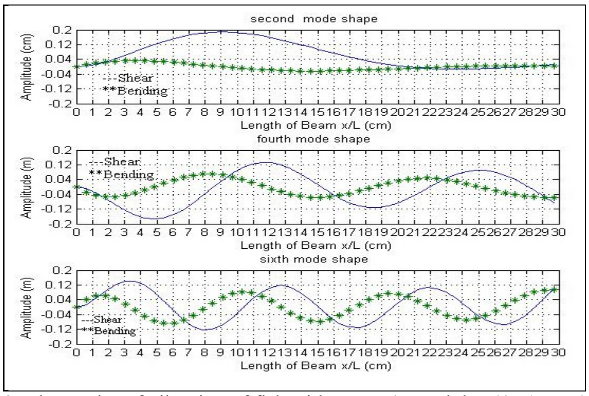

Fig. 3: The modes of vibration of fish with Young's modulus (4.5175E5) and moment of inertia (8.48275E-6)

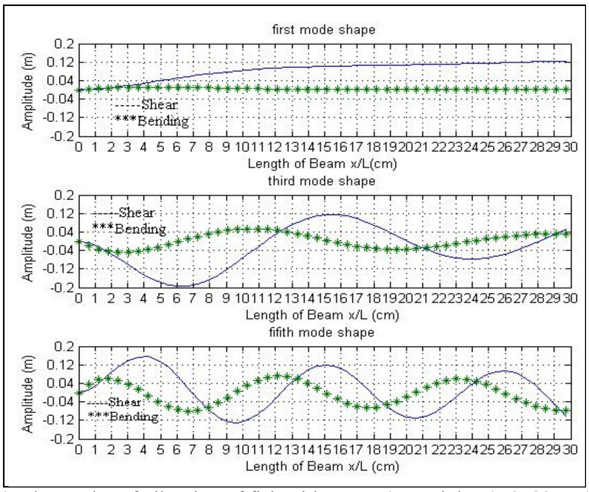

Fig. 4: The modes of vibration of fish with Young's modulus (5.05825E5) and moment of inertia (1.655E-5)

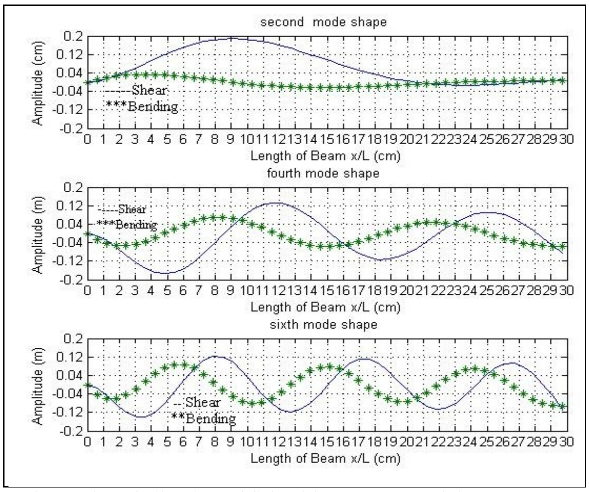

Fig. 5: The modes of vibration of fish with Young's modulus (5.05825E5) and moment of inertia (1.655E-5)

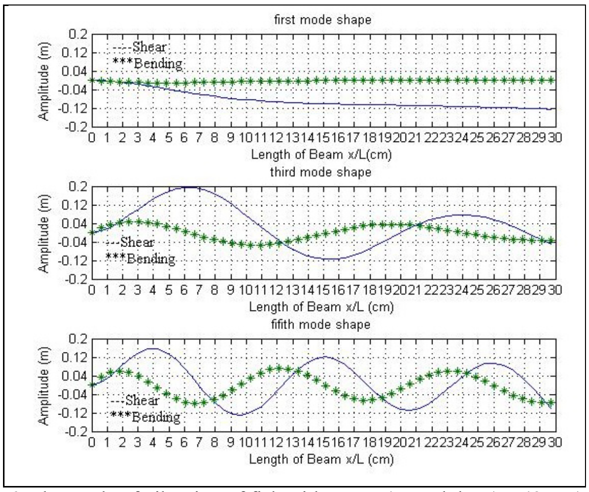

Fig. 6: The mode of vibration of fish with Young's modulus (5.5425E5) and moment of inertia (2.4619E-5)

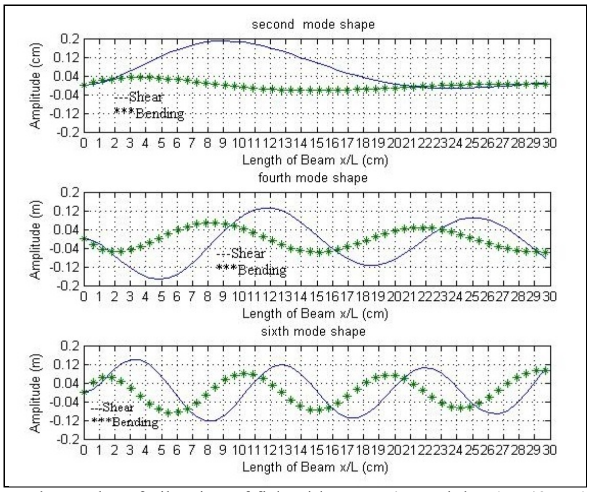

Fig. 7: The modes of vibration of fish with Young's modulus (5.5425E5) and moment of inertia (2.4619E-5)

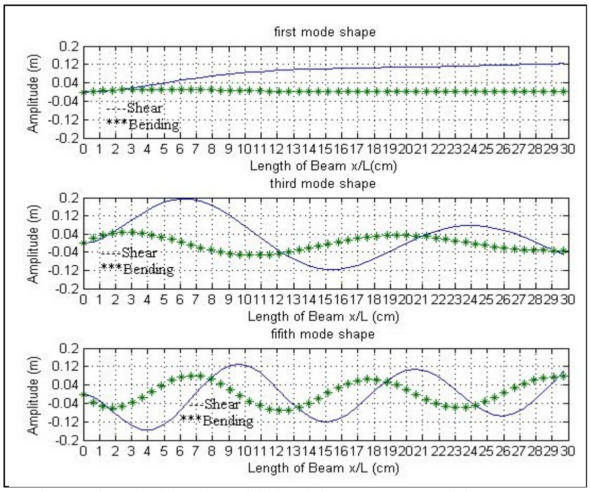

Fig. 8: The modes of vibration of fish with Young's modulus (6.0267E5) and moment of inertia (3.227E-5)

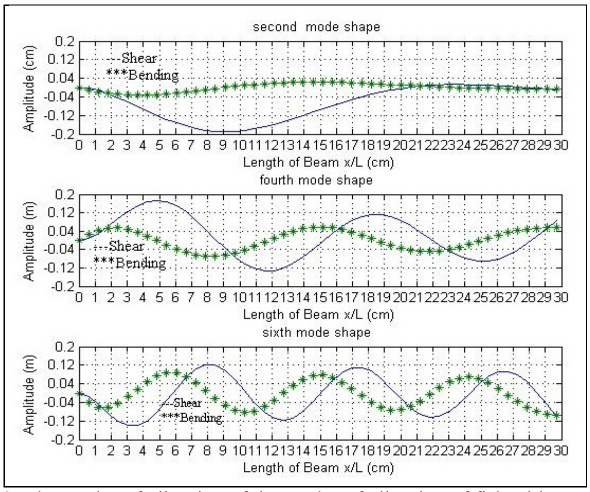

Fig. 9: The modes of vibration of the modes of vibration of fish with Young's modulus (6.0267E5) and moment of inertia (3.227E-5)

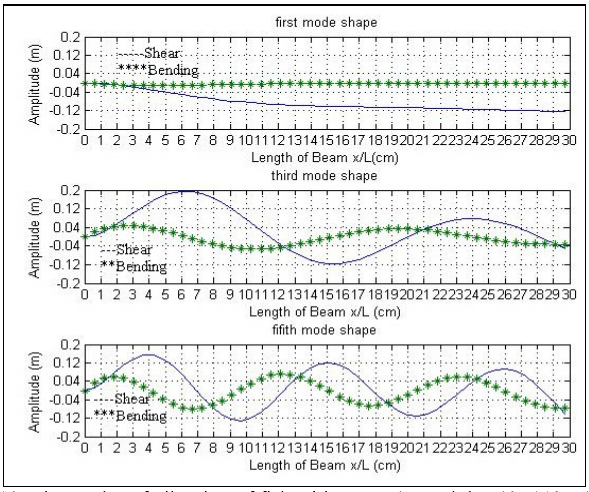

Fig. 10: The modes of vibration of fish with Young's modulus (6.5112E5) and moment of inertia (4.077273e-5)

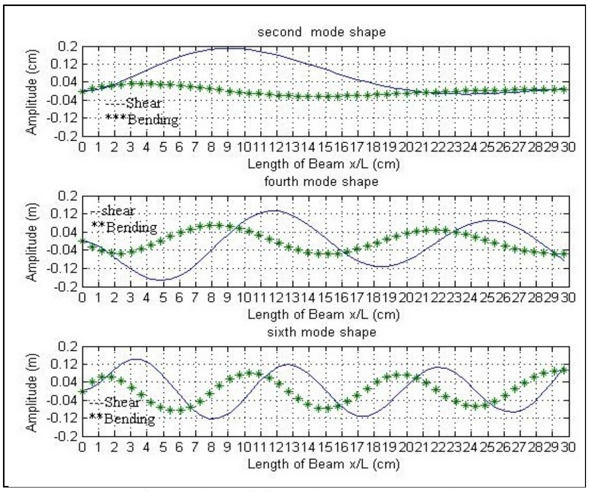

Fig. 11: The modes of vibration of fish with Young's modulus (6.5112E5) and moment of inertia (4.077273e-5)

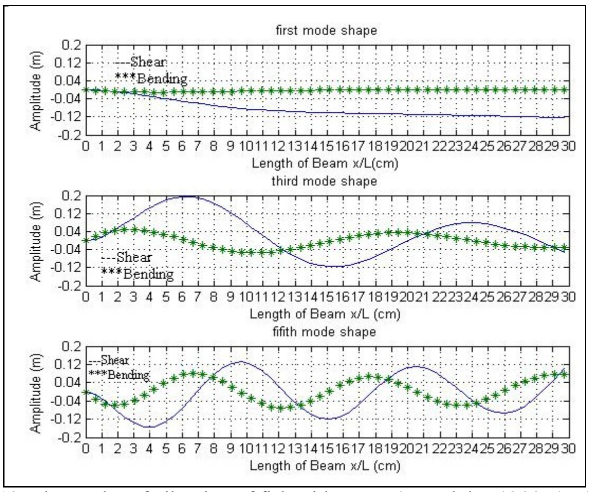

Fig. 12: The modes of vibration of fish with Young's modulus (6.9954E5) and moment of inertia (4.8845E-5)

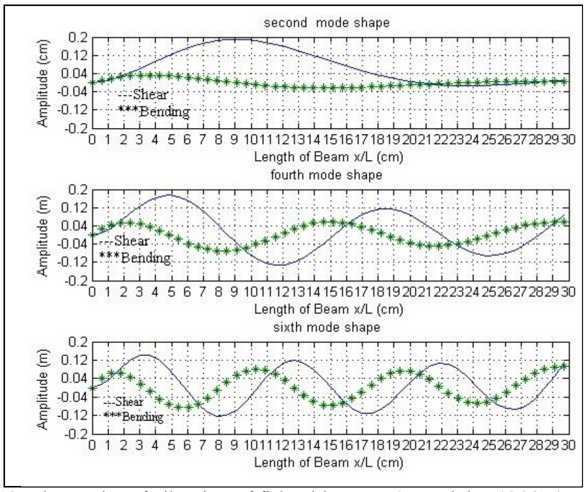

Fig. 13: The modes of vibration of fish with Young's modulus (6.9954E5) and moment of inertia (4.8845E-5)

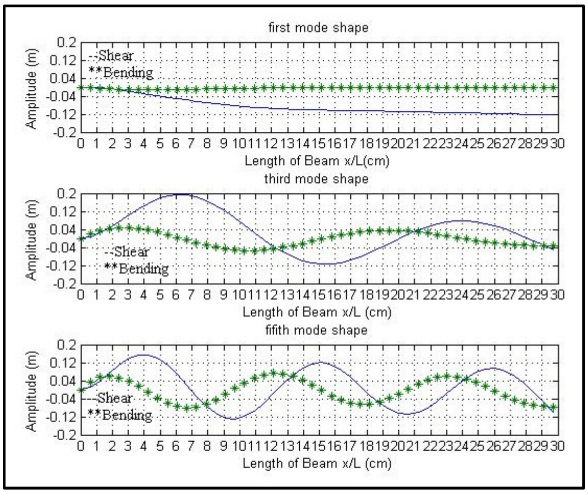

Fig. 14: The modes of vibration of fish with Young's modulus (7.47976E5) and moment of inertia (5.6918E-5)

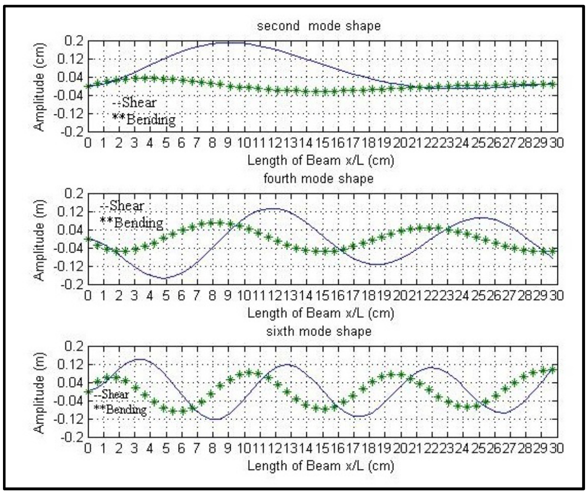

Fig. 15: The modes of vibration of fish with Young's modulus (7.47976E5) and moment of inertia (5.6918E-5)

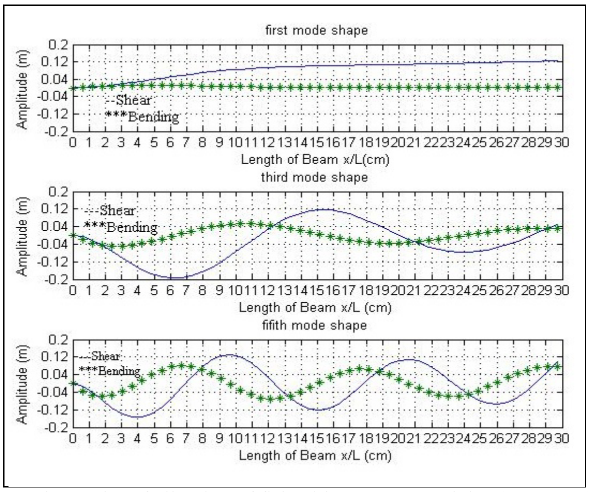

Fig. 16: The modes of vibration of fish with Young's modulus (7.9639E5) and moment of inertia (6.5E-5)

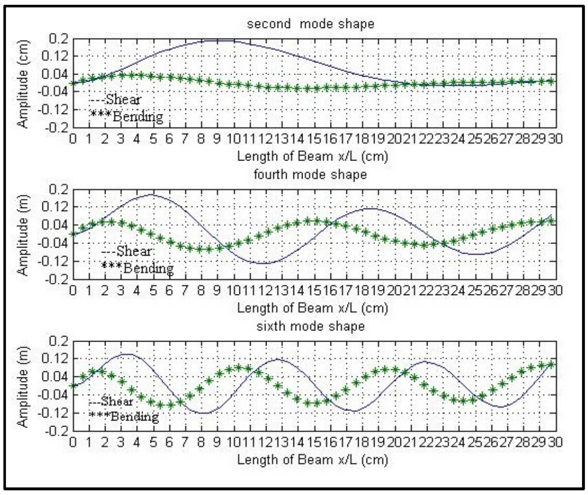

Fig. 17: The modes of vibration of fish with Young's modulus (7.9639E5) and moment of inertia (6.5E-5)

VIII. VARIATION OF SECTIONAL AREA MOMENT OF INERTIA VS AMPLITUDE

The variation of amplitude vs sectional moment of inertia is listed in Table 1.

Table 1: Variation of moment of inertia of robotic fish.

Variation of the sectional area moment of inertia (m^4) *E-5	Amplitude of sixth mode of vibration of the TM beam (m)	Amplitude of second mode of vibration of the TM beam (m)	Amplitude of first mode of vibration of the TM beam (m)
0.84827	0.09, -0.09	0.01, -0.01	0
1.655	0.09, -0.09	0.03, -0.03	0
2.4619	0.09, -0.1	0.04, -0.035	0
3.227	0.09, -0.09	0.035, -0.04	0
4.0772	0.09, -0.09	0.04, -0.035	0.01, -0.01
4.8845	0.1, -0.1	0.04, -0.035	0.01, -0.01
5.6918	0.11, -0.09	0.04, -0.035	0.01, -0.01
6.5369	0.12, -0.09	0.035, -0.035	0.01, -0.01

IX. VARIATION OF AMPLITUDE VS YOUNG'S MODULUS

The variation of amplitude vs Young's modulus of robotic fish is shown in Table 2. In our simulation model, we assume that the head of the fish is clamped, the fish is neutrally buoyant and confined to X, Y and Z planes. Furthermore, the flexible tail behaves like a TB and this implies that all points along the length of tail moves in z direction only and the displacement and slope of the tail with respect to x and y axes are small. We can observe from Table 2 that the amplitude in all the modes increase with increase in E. This is result of the flexibility that increases with an increase in E.

Table 2: Variation of Young's modulus of robotic fish.

Variation of Young's modulus (N/m^2) *E5	Amplitude of sixth mode of vibration of the TM beam (m)	Amplitude of second mode of vibration of the TM beam (m)	Amplitude of first mode of vibration of the TM beam (m)
4.5175	0.09, -0.09	0.01,-0.01	0, -0
5.05825	0.09, -0.09	0.03,-0.03	0, -0
5.5425	0.09, -0.1	0.04,-0.035	0.01, -0.01
6.0267	0.09, -0.09	0.035,-0.04	0, -0
6.511	0.09, -0.09	0.04,-0.035	0.01, -0.01
6.995	0.1, -0.1	0.04,-0.035	0, -0
7.479	0.11, -0.09	0.04,-0.035	0, -0
7.9639	0.12, -0.09	0.035,-0.035	0.01, -0.01

X. MODELING OF AMPLITUDE AND THRUST

A. For Sinusoid Motion

In un-dulatory motion, the amplitude of waves tends to increase as the waves pass posteriorly along the body and following [10-11] this can be formulated:

$$y = b(x)\sin k(x + V\,wt) \quad \text{.......................... (7)}$$

$$F_T = C_T (V_T \, \text{Sin}\theta + V_N \, \text{Sin}\theta)\, dx \quad \text{.................. (8)}$$

$$F_N = C_N (V_T \, \text{Cos}\theta - V_N \, \text{Sin}\theta)\, dx \quad \text{.............. (9)}$$

and in equations (7-9), as shown in Fig. 18, the propulsive components F_N & F_L along the axis of propulsion are $F_N \, \text{Sin}\theta$, $F_T \, \text{Cos}\theta$:

$$dF = F_N \, \text{Sin}\theta - F_T \text{Cos}\theta \quad \text{.............. (10)}$$

and the integration dF of will result into F. Furthermore,

F =Force which is exerted on the water (N),

F_T =Tangential force (N),

F_N =Normal force (N),

V_T = Velocity of wave in the tangential component (m/s),

V_N = Velocity of wave in normal component (m/s),

V_W = Wave velocity of tail (m/s),

V_X = Propulsive velocity in x direction (m/s),

b = Amplitude of wave created by fish motion,

C_N = Coefficient of lift, and

C_T = Coefficient of drag.

Now, we formulate:

$$F = \frac{2\pi^2 b^2 V_W}{\lambda}(C_N - C_T) - C_T \lambda V_X \quad (11)$$

$$y = b(x)\sin k(x + Vwt) \quad (12)$$

And, for small and large amplitudes following [11], we compute the thrust:

$$F = (V_W I - V_x J) \quad (13)$$

$$I = \int_0^{\lambda}\left[\frac{\frac{4\pi^2 b^2}{\lambda^2}\cos^2\frac{2\pi}{\lambda}(x + V_W t)}{[1 + \frac{4\pi^2 b^2}{\lambda^2}\cos^2\frac{2\pi}{\lambda}(x + V_W t)]^{1/2}}\right]dx \quad (14)$$

$$J = \int_0^{\lambda}\left[\frac{\frac{8\pi^2 b^2}{\lambda^2}\cos^2\frac{2\pi}{\lambda}(x + V_W t)}{[1 + \frac{4\pi^2 b^2}{\lambda^2}\cos^2\frac{2\pi}{\lambda}(x + V_W t)]^{1/2}}\right]dx \quad (15)$$

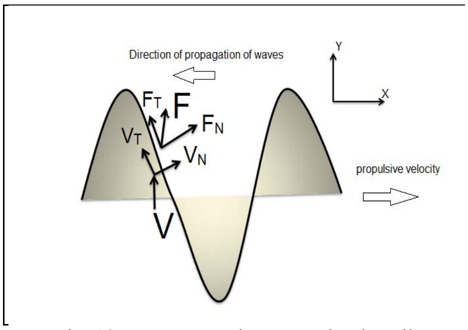

Fig. 18: Force exerted on water by the tail

The computed thrust with various wave velocities is shown in Table 3.

Table 3: Computed thrust with various wave velocities

Thrust delivered by the fish (mili N)	Velocity of wave relatively to the head or wave velocity (cm/s)
0.5655	15.05149
1.78134	19.637
1.8319	20.0431

Also, in simulation model, the following conditions are imposed:

- The tail needs to conform to that of a sine wave, the changes in curvature and the rate of transverse displacement about the axis of progression symmetrical.

- The amplitude can change as a wave passes along the tail and the propulsive properties of the latter are expected to be closely similar to those of a tail generating waves of the same average amplitude.

- When the phase difference increases, the 'figure of eight - ∞' motion becomes more prominent. This motion has also been observed in swimming fish and the fin that generate this motion yields larger thrust compared with the fin that did not generate a figure-eight motion.

The variation of mode contribution with respect to thrust with different velocities is shown in Fig. 19.

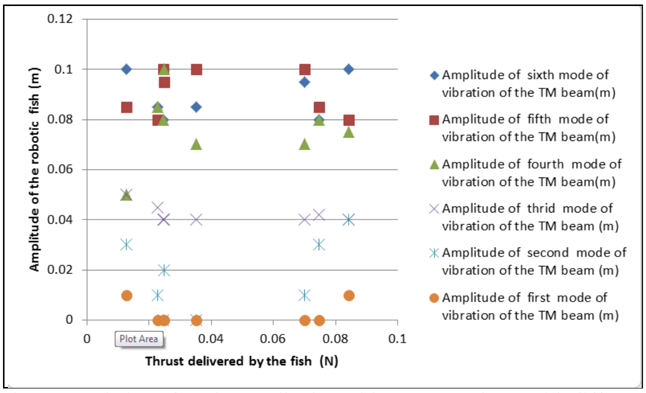

Fig. 19: Variation of mode contribution with respect to thrust with different velocities

XI. RELATION BETWEEN PROPULSIVE MODE AND THRUST

As per [11], the bending waves passing along the length of an elongated body can propel an animal forward if the body pushes laterally against its surroundings with a force that is greater than the force required to drag the body parallel to its length, where momentum is insignificant and the resistances are purely viscous. In our idea, the bio-mimetic robotic fish propels itself through the water at a speed that is a function of six parameters and they are:

- frequency of the waves,
- square of the amplitude of the waves,
- wave-length,
- difference between the coefficients of normal and tangential resistance, and
- length of the tail.

In many fishes, the amplitude of the waves tends to increase as the waves pass posteriorly along the body. This means that the propulsive speed of a bio-mimetic fish can be expressed in terms of the amplitude, wave-length and frequency of the waves passing down the tail of a fish and the amplitude can change as a wave passes along the tail. In undulatory propulsion, the equation for forward swimming velocity is a function of the frequency, amplitude and wavelength of the bending waves. The magnitude of the forward tangential thrust imparted to the body depends on the magnitude of the internally generated bending couples. In an undulating mode, the fish swims forward and the waves passing down the body move backwards relative to the ground and the maximum rate of the fish progression is less than the rate at which the waves are propagated backwards over the body. The propulsive power of a wave increases with an increase of amplitude and decreases with an increase of wavelength.

XII. MODELLING AND NUMERICAL SIMULATION DETAILS

(A) Variation of small and large amplitude in fish

The variation of thrust vs the small amplitude of caudal fin is shown in Fig. 20. And, the variation of thrust vs the large amplitude of caudal fin is shown in Fig. 21.

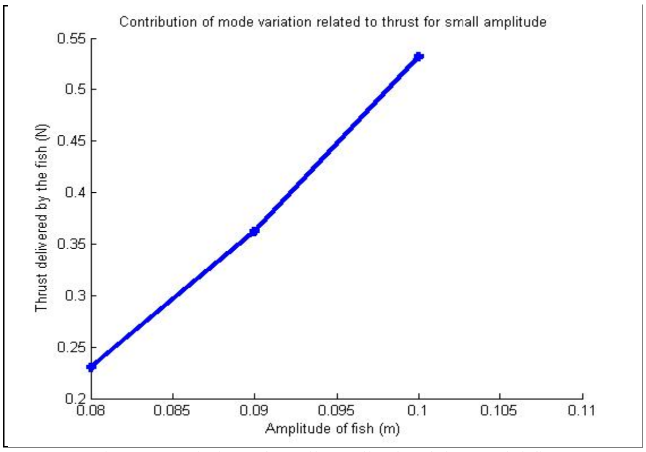

Fig. 20: Variation of small amplitude of the caudal fin

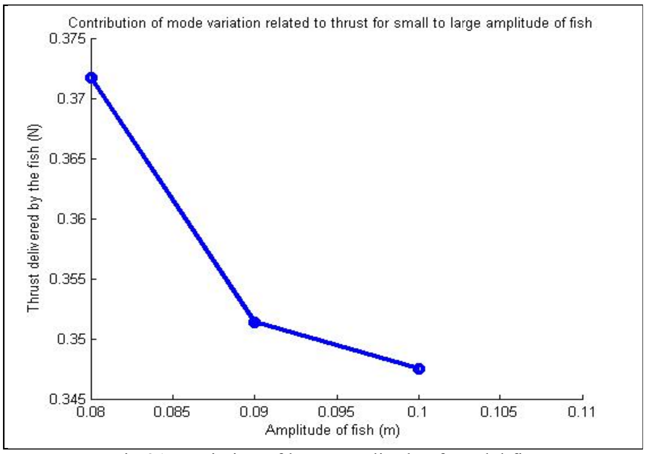

Fig 21: Variation of large amplitude of caudal fin

We can note from Figs. 20 and 21 that the thrust decreases with large amplitude with different wave velocities.

(B) Validation

We use the simulation results of Equations (7-15) and compare them with the analytical expressions of [15]. The comparison is listed in Table 4. And, we can see that the simulation model of this paper matches well with [14].

Table 4: Validation of the present computer simulation model with [14].

Velocity of wave relative to head (cm/s)	Amplitude obtained by simulation (m)	Amplitude computed with analytical expressions (Separability of drag and thrust in undulatory animals and machines)
19.637	0.061	0.056
20.0106	0.082	0.078
28.849	0.15	0.1

XIII. SMART FISH

In practice, the proper placement and subsequent gain through the use of Macro Fibre Composite (MFC) patches in TB beam is difficult. However, the MFC patches can be attached along the sides of the TB beam, and the frequency adjustments of MFC in the caudal fin can be operated independently. The idea is that the amplitude is highest when the two MFC patches operate in phase equilibrium and are at close to resonance. The oscillation can be achieved by subjecting the piezo-fibers to an Alternate Current (AC) signal produced by a function generator and this causes the piezo-fibers to expand and contract in cyclic order. By tuning the input frequency with fundamental frequency of the MFC-tail, the small movement of the patch can cause large oscillations at the free end of the robotic tail. The mode shapes of the piezo tail are not perfectly linear and therefore the actuators need to be positioned in the region. The details of our bio-mimetic fish are listed below. And, the schematic and basic functional design is shown in Fig. 22.

(A) Details of the bio-mimetic fish

Description	Length of the fish (cm)	Width of the fish (cm)	Weight of fish
Smart fish	30 cm	6 cm	0.5 Kg

(A) Design Model of the Smart fish

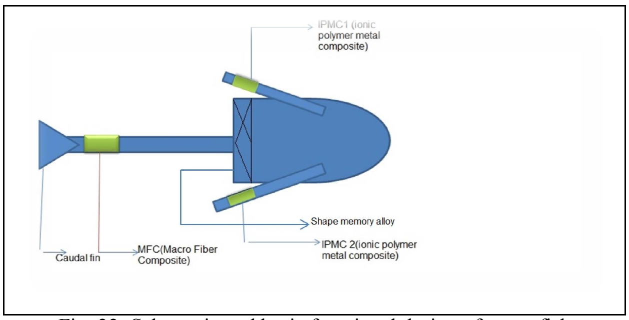

Fig. 22: Schematic and basic functional design of smart fish

Fig. 23 shows that MFC beam can be actuated by applying voltage to the MFC and it is constructed using piezo-fibers which allow the orthogonal vibration modes in the structure. It can give a travelling wave type results and that improves the propulsive mode of the caudal fin. The MFC can produce significantly more strain energy than that of a typical piezo-ceramic actuator due to the use of inter-digitized electrodes that capitalize on the higher piezoelectric 'd33' coefficient, one MFC patch can sufficiently excite global modes.

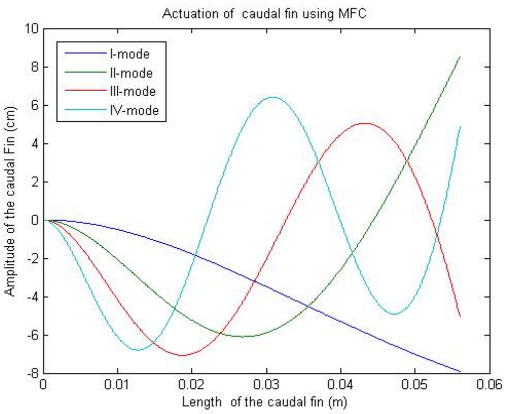

Fig 23: Actuation of caudal fin using MFC

XIV. CONCLUSIONS

We presented a computer simulation model to study the bio-mimetic fish modeled as a compliant beam. In the model, we determined the natural frequencies of the fish and then computed and characterized the mode shapes and related them to propulsive thrust.

In our application of model, we focused on design of propulsion systems with compliant bodies for bio-mimetic locomotion in marine environments and in this regard we have presented a conceptual design. In future, we plan to design the compliant bodies in natural frequency modes (i.e. the mode that most resembles the desired kinematics) and match range of natural frequencies that are energy efficient.

The presented results have been validated with earlier work of [14], and the results show that presented simulation model computes mode shape and the resultant thrust with reasonable accuracy. Now, we shall focus on experimental studies of compliant bodies for bio-mimetic locomotion and this is currently being investigated by the authors.

REFERENCES

[1] P. V.y Alvarado, "Design of Biomimetic Compliant Devices for Locomotion in Liquid Environments*",* PhD Thesis, MIT, USA, 2007.

[2] M. S. Triantafillou and G. S. Triantafyllou, "An efficient swimming machine", *Scientific American*, 272 (3), pp. 64-70, 1995.

[3] W. Thomson, *Theory of Vibration with Applications*, 4th edition, CRC Press, USA.

[4] D. Sun, J. K. Mills, J. J. Shan, and S. K. Tso, "A PZT actuator control of a single-link flexible manipulator based on linear velocity feedback and actuator placement", *Mechatronics*, vol. 14, no. 4, pp. 381-401, 2004.

[5] S. Devasia, B. Paden, and E. Bayo, "Piezoelectric actuator design for vibration suppression: Placement and sizing", in *Proc. of the 31st Conference on Decision & Control*, pp. 1367-1372, 1992.

[6] S. Moheimani and T. Ryall, "Considerations on placement of piezo-ceramic actuators that are used in structural vibration control", in *Proc. of the 38th Conference on Decision & Control*, pp. 1187-1193, 1999.

[7] D. Sun and J. K. Milles, "Study on piezoelectric actuators in control of a single link flexible manipulator", in *Proc. IEEE Int. Conf. on Robotics and Automation* (Detroit, MI) (Piscataway, NJ: IEEE), vol. 2, pp. 849-854, 1999.

[8] F. R. Harden Jones, "Tail beat frequency, amplitude, and swimming speed of a shark tracked by sector scanning sonar", *ICES J. Mar. Sci.*, vol. 35, no. 1, pp. 95-97, 1973.

[9] S. Sorrentino, S. Marchesiello, and B. A. D. Piombo, "A new analytical technique for vibration analysis of non-proportionally damped beams", *Journal of Sound and Vibration*, vol. 265, no. 4, pp. 765-782, 2003.

[10] E. F. Crawley and J. Deluis, "Use of piezoelectric actuators as elements of intelligent structures", *AIAA Journal*, vol. 25, no. 10, pp. 1373-1385, 1987.

[11] J. Gray, "Undulatory Propulsion", *Quarterly Journal of Microscopical Science*, vol. 94, part 4, pp. 551-578, 1953.

[12] G. K. Ananthasuresh, S. Kota, "Designing compliant mechanisms", *ASME Mechanical* Engineering, November, 1995, pp. 93-96.

[13] L. L. Howell, Compliant Mechanisms, Wiley-IEEE, 2001.

[14] R. Bale, A. A. Shirgaonkar, I. D. Neveln, A. P. S. Bhalla, M. A. MacIver and N. A. Patankar, "Separability of drag and thrust in undulatory animals and machines", Nature Scientific Reports 4, 7329, (2014), doi:10.1038/srep07329